Rapid Communications

Exact large deviation statistics and trajectory phase transition of a deterministic boundary driven cellular automaton

Berislav Buča,[1] Juan P. Garrahan,[2] Tomaž Prosen,[3] and Matthieu Vanicat[3]

[1]*Clarendon Laboratory, University of Oxford, Parks Road, Oxford OX1 3PU, United Kingdom*

[2]*School of Physics and Astronomy and Centre for the Mathematics and Theoretical Physics of Quantum Non-Equilibrium Systems, University of Nottingham, Nottingham NG7 2RD, United Kingdom*

[3]*Faculty of Mathematics and Physics, University of Ljubljana, Jadranska 19, SI-1000 Ljubljana, Slovenia*

(Received 14 January 2019; revised manuscript received 19 June 2019; published 19 August 2019)

We study the statistical properties of the long-time dynamics of the rule 54 reversible cellular automaton (CA), driven stochastically at its boundaries. This CA can be considered as a discrete-time and deterministic version of the Fredrickson-Andersen kinetically constrained model (KCM). By means of a matrix product ansatz, we compute the exact large deviation cumulant generating functions for a wide range of time-extensive observables of the dynamics, together with their associated rate functions and conditioned long-time distributions over configurations. We show that for all instances of boundary driving the CA dynamics occurs at the point of phase coexistence between competing active and inactive dynamical phases, similar to what happens in more standard KCMs. We also find the exact finite size scaling behavior of these trajectory transitions, and provide the explicit "Doob-transformed" dynamics that optimally realizes rare dynamical events.

DOI: 10.1103/PhysRevE.100.020103

Introduction. Classical systems which evolve stochastically subject to constraints display complex dynamics, often beyond what can be anticipated simply from their static properties. This is what occurs in the presence of excluded volume interactions, such as in simple exclusion processes [1,2], or when configuration space is restricted, such as in dimer coverings [3,4], or in systems where dynamical rules are subject to *kinetic constraints*, as for example in kinetically constrained models (KCMs) of glasses [5,6]. Constrained dynamics is also proving increasingly relevant to quantum many-body systems, including problems such as slow thermalization and nonergodicity in the absence of disorder [7–11], operator spreading and entanglement growth [12–19], and in the dynamics of ensembles of Rydberg atoms [20–22].

Complex collective dynamics must be characterized through the statistical properties of dynamical observables, something which can be readily done by means of large deviation (LD) techniques [23–26]. This allows to study ensembles of trajectories of the dynamics as one would study ensembles of configurations in equilibrium statistical mechanics. Among other things, the dynamical LD approach reveals in many systems the existence of competing *dynamical phases* and the corresponding phase transitions between them, as for example in KCMs [24,25], exclusion processes [27–30], dimer models [31], and several other classical [32–35] and quantum [36] systems. This rich phase structure of trajectory space is what underlies the complex dynamics of these systems.

Here we generalize the above ideas to systems whose (bulk) dynamics is *deterministic* and *reversible*. We consider specifically the "rule 54" cellular automaton (CA) of Ref. [37] (RCA54). The local rules that define the interactions of this CA (see below) are similar to the kinetic constraints of the simplest of KCMs, the (one-spin facilitated) Fredrickson-Andersen (FA) model [5,38,39]. As such the RCA54 is referred to also as the "Floquet-FA" model [16] since it can be considered a synchronous, discrete, and deterministic version of the FA model. (The RCA54 is also related to the ERCA 250R of Takesue [40].) A remarkable property of the RCA54 is that it is *integrable* [41] and, in the presence of stochastic driving at its boundaries, one can obtain exactly its (in general nonequilibrium) steady-state distribution [41,42], certain decay modes [43], and dynamical structure factors [44] in terms of matrix product states.

In this Rapid Communication we compute the *exact large deviation statistics* of the boundary driven RCA54 by generalizing the methods of Refs. [41–44]. Via a novel inhomogeneous matrix product ansatz we obtain the exact cumulant generating functions and rate functions of a broad class of time-extensive observables of the dynamics. We prove the existence of distinct active and inactive dynamical phases, with the dynamics of the RCA54 occurring at the phase transition point. To our knowledge, our findings here represent the only exact results for LDs in interacting models beyond those for simple exclusion processes [27,45–51] (and related hard-core Brownian particle models [52]), and the first for bulk-deterministic systems. Previous work for bulk-deterministic systems focused on stationarity states (e.g., [53]). Our approach goes beyond effective hydrodynamic description [54] and accesses the full microscopic dynamics and the matrix product ansatz introduced allows us to calculate the large deviations of *arbitrary* two-site observables. It includes nontrivial correlations in contrast to previous results for product states [55].

Model. We consider a system defined by binary variables $n_i \in \{0, 1\}$ (up/down state) on sites $i \in \{1, \ldots, N\}$ of a lattice with even size N. A configuration at time t is described by a

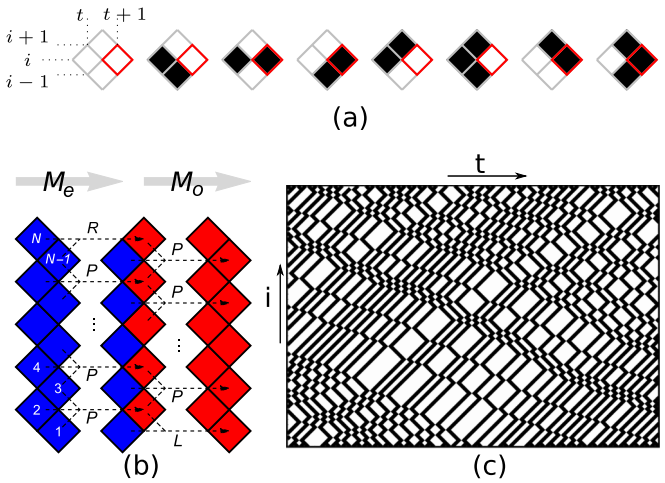

FIG. 1. Boundary-driven RCA54: (a) Deterministic local dynamical rules for bulk dynamics. (b) Action of the propagator in the two half-time steps. (c) A typical trajectory of the model for $(N, T) = (100, 75)$ and stochastic boundaries with $(\alpha, \beta, \gamma, \delta) = (1/3, 1/8, 1/2, 2/5)$.

binary string $\boldsymbol{n}^t = (n_1^t, n_2^t, \ldots, n_N^t)$. The dynamics in the bulk is given by the discrete, deterministic RCA54 [37], while the dynamics on the boundary sites is stochastic [41,43].

The update rule is decomposed into two Floquet-like half-time steps. During the first half-time step, $\boldsymbol{n}^t \to \boldsymbol{n}^{t+1/2}$, only even sites are updated, so that $n_i^{t+1/2} = n_i^t$ for i odd. For all i even with $2 \leqslant i \leqslant N-2$, the evolution of n_i^t is deterministic through the relation $n_i^{t+1/2} = \chi(n_{i-1}^t, n_i^t, n_{i+1}^t)$, where $\chi(n, n', n'') = n + n' + n'' + nn'' \mod 2$ is the rule-54 function [37] [see Fig. 1(a)]. This local update rule is similar to the constraint of the FA model: A site can flip only if at least one of its nearest neighbors is in the up state [38]. The last site is updated stochastically depending on the state of its neighbor: $n_N^{t+1/2} = 0$ with probability $\gamma + n_{N-1}^t(\delta - \gamma)$ or $n_N^{t+1/2} = 1$ otherwise. In the second half-time step, $\boldsymbol{n}^{t+1/2} \to \boldsymbol{n}^{t+1}$, for even sites we have $n_i^{t+1} = n_i^{t+1/2}$, while odd sites in the bulk evolve deterministically with rule-54, $n_i^{t+1} = \chi(n_{i-1}^{t+1/2}, n_i^{t+1/2}, n_{i+1}^{t+1/2})$. The first site is updated stochastically, with $n_1^{t+1} = 0$ with probability $\alpha + n_2^{t+1/2}(\beta - \alpha)$ or $n_1^{t+1} = 1$ otherwise.

The above rules define a discrete-time, irreducible, and nonreversible (due to the stochastic boundaries) Markov process. Physically it models a gas of solitons stochastically emitted from reservoirs at the boundaries, propagating at constant unit velocity in the bulk and interacting pairwise through a one-time step delay [41–43]. Depending on the boundary rates, the system is driven out-of-equilibrium by the reservoirs leading to a net flow of solitons in the stationary state.

We define $p_{\boldsymbol{n}}^t$ to be the probability that $\boldsymbol{n}^t = \boldsymbol{n}$ and $\boldsymbol{p}^t = \sum_{n_1,n_2,\ldots,n_N \in \{0,1\}} p_{\boldsymbol{n}}^t \, e_{n_1} \otimes e_{n_2} \otimes \cdots \otimes e_{n_N}$ the associated probability vector in $(\mathbb{R}^2)^{\otimes N}$ (where e_0 and e_1 denote the elementary basis of $\mathbb{R}^2$). The master equation can be written as $\boldsymbol{p}^{t+1} = M\boldsymbol{p}^t$ where the Markov matrix $M = M_o M_e$ is expressed as the product of two operators associated with the even and odd half-time steps [see Fig. 1(b)],

$$M_e = P_{123}P_{345}\cdots P_{N-3,N-2,N-1}R_{N-1,N},$$
$$M_o = L_{12}P_{234}P_{456}\cdots P_{N-2,N-1,N}. \tag{1}$$

The subscripts indicate on which sites of the lattice the operators are acting nontrivially. The operator P is the 8×8 permutation matrix (acting on three sites) that enforces the dynamical rule in the bulk, with elements $P_{nn'n''}^{mm'm''} = \delta_{n,m}\delta_{\chi(nn'n''),m'}\delta_{n'',m''}$ where $\delta_{n,m}$ is the Kronecker symbol. The operators L and R are the 4×4 stochastic matrices for the boundary processes of the first and last site, respectively. A typical trajectory of the RCA54 is shown in Fig. 1(c). For further details of the model see [41–43,56].

Large deviations of time-integrated observables. We are interested in the statistics of general (possibly inhomogeneous) space- and time-extensive observables of the form

$$\mathcal{O}_T = \sum_{t=0}^{T-1}\sum_{j=1}^{N-1}\left[f_j\left(n_j^t, n_{j+1}^t\right) + g_j\left(n_j^{t+1/2}, n_{j+1}^{t+1/2}\right)\right] \tag{2}$$

in the large time T limit. These are dynamical (or trajectory) observables as they depend on the full time history $(\boldsymbol{n}^0, \boldsymbol{n}^{1/2}, \boldsymbol{n}^1, \ldots, \boldsymbol{n}^{T-1/2})$. An example is the time-integrated number of up sites (which is not conserved in the RCA54) corresponding to $f_j(n, n') = (n + n')/2$ and $g_j(n, n') = 0$.

For large T the probability of $\mathcal{O}_T$ has a LD form, $P_T(\mathcal{O}) = \langle\delta(\mathcal{O} - \mathcal{O}_T)\rangle \sim_{T\to\infty} e^{-T\varphi_N(\mathcal{O}_T/T)}$, where $\varphi_N(x)$ is the *rate function* (where the subscript indicates its size dependence). The moment generating function also has a LD form, $Z_T(s) = \langle e^{-s\mathcal{O}_T}\rangle \sim e^{T\theta_N(s)}$, where $\theta_N(s)$ is called the *scaled cumulant generating function* (SCGF), as its derivatives at $s = 0$ correspond to the cumulants of $\mathcal{O}_T$ divided by time. The LD functions play the role of free energies for trajectories and are related by a Legendre transform, $\theta_N(s) = -\min_x[sx + \varphi_N(x)]$.

To obtain the SCGF we deform, or *tilt*, the Markov matrix [26]: We define $M(s) = M_o\,G(s)\,M_e\,F(s)$, where we have introduced the diagonal operators $F_{\boldsymbol{n},\boldsymbol{n}'}(s) = \delta_{\boldsymbol{n},\boldsymbol{n}'}\prod_{i=1}^{N-1} f_{n_i,n_{i+1}}^{(i)}$ and $G_{\boldsymbol{n},\boldsymbol{n}'}(s) = \delta_{\boldsymbol{n},\boldsymbol{n}'}\prod_{i=1}^{N-1} g_{n_i,n_{i+1}}^{(i)}$, with the shorthand notation $f_{n,n'}^{(i)} = e^{-sf_i(n,n')}$ and $g_{n,n'}^{(i)} = e^{-sg_i(n,n')}$. We then have that $\theta_N(s) = \ln\lambda(s)$, where $\lambda(s)$ is the largest real eigenvalue of $M(s)$.

Exact results from matrix ansatz. During the last decades, a technique called matrix ansatz has proven to be very efficient for deriving exact results in out-of-equilibrium systems. It has been introduced to compute analytically the stationary state of Markov chains [57] (see also [58,59] for recent developments) and has later on been used to compute deformed ground state [48,60], eigenvectors [43,61], or time evolution of particular initial states [44]. We use it here to compute the ground state of the tilted Markov operator $M(s)$. Following the approach of [41,43], our strategy is to look for vectors $\boldsymbol{p}$ and $\boldsymbol{p}'$ such that $M_eF(s)\boldsymbol{p} = \lambda_R(s)\boldsymbol{p}'$ and $M_oG(s)\boldsymbol{p}' = \lambda_L(s)\boldsymbol{p}$. It then follows that $\lambda(s) = \lambda_R(s)\lambda_L(s)$ is the dominant eigenvalue of the tilted Markov operator, $M(s)\boldsymbol{p} = \lambda(s)\boldsymbol{p}$.

It turns out that one can construct four pairs of site-dependent 3×3 matrices $W_n^{(j)}$, $V_n^{(j)}$, $X_n^{(j)}$, $Y_n^{(j)}$ [56] which

satisfy the inhomogeneous bulk relations, for j even:

$$f^{(j-1)}_{nn'} f^{(j)}_{n'n''} W^{(j-1)}_{n} W^{(j)}_{n'} X^{(j+1)}_{n''} = X^{(j-1)}_{n} V^{(j)}_{\chi(nn'n'')} V^{(j+1)}_{n''},$$
$$g^{(j-2)}_{nn'} g^{(j-1)}_{n'n''} X^{(j-2)}_{n} V^{(j-1)}_{n'} V^{(j)}_{n''} = W^{(j-2)}_{n} W^{(j-1)}_{\chi(nn'n'')} X^{(j)}_{n''},$$

as well as six row 3-vectors $\langle l_n|$, $\langle l'_{nn'}|$ and six column 3-vectors $|r_{nn'}\rangle$, $|r'_n\rangle$, satisfying the boundary equations

$$f^{(1)}_{nn'} f^{(2)}_{n'n''} \langle l_n| W^{(2)}_{n'} X^{(3)}_{n''} = \langle l'_{n\chi(nn'n'')}| V^{(3)}_{n''},$$
$$\sum_{m,m'=0,1} R^{mm'}_{nn'} f^{(N-1)}_{mm'} |r_{mm'}\rangle = \lambda_{\mathrm{R}} X^{(N-1)}_{n} |r'_{n'}\rangle,$$
$$\sum_{m,m'=0,1} L^{mm'}_{nn'} g^{(1)}_{mm'} \langle l'_{mm'}| = \lambda_{\mathrm{L}} \langle l_n| X^{(2)}_{n'},$$
$$g^{(N-2)}_{nn'} g^{(N-1)}_{n'n''} X^{(N-2)}_{n} V^{(N-1)}_{n'} |r'_{n''}\rangle = W^{(N-2)}_{n} |r_{\chi(nn'n'')n''}\rangle.$$

These equations provide a cancellation scheme implying that an eigenvector of M, specifically vectors $\boldsymbol{p}$ and $\boldsymbol{p}'$, take the matrix product form

$$p_{n_1,\ldots,n_N} = \left\langle l_{n_1} \right| W^{(2)}_{n_2} W^{(3)}_{n_3} \cdots W^{(N-3)}_{n_{N-3}} W^{(N-2)}_{n_{N-2}} \left| r_{n_{N-1}n_N} \right\rangle,$$
$$p'_{n_1,\ldots,n_N} = \left\langle l'_{n_1 n_2} \right| V^{(3)}_{n_3} V^{(4)}_{n_4} \cdots V^{(N-2)}_{n_{N-2}} V^{(N-1)}_{n_{N-1}} \left| r'_{n_N} \right\rangle. \quad (3)$$

An explicit expression of the matrices and boundary vectors in the three-dimensional auxiliary space are provided in [56]. The eigenvalue $\lambda = \lambda_{\mathrm{L}}\lambda_{\mathrm{R}}$ is proven to be the dominant root of a polynomial of order 4:

$$\lambda^4 - \alpha\gamma\mathfrak{a}_N\lambda^3 - \omega\mathfrak{a}_N^2\lambda^2 - \beta\delta\xi\mathfrak{a}_N^3\lambda + \eta\mathfrak{a}_N^4 = 0, \quad (4)$$

with

$$\omega = \mathfrak{b}_N(1-\alpha)(1-\delta)\beta'\gamma' + \mathfrak{c}_N(1-\beta)(1-\gamma)\alpha'\delta',$$
$$\xi = \mathfrak{b}_N\mathfrak{c}_N(1-\alpha)(1-\beta)(1-\gamma)(1-\delta)\frac{\alpha'\beta'\gamma'\delta'}{\widetilde{\alpha}\widetilde{\beta}\widetilde{\gamma}\widetilde{\delta}},$$
$$\eta = (\alpha\beta - \widetilde{\alpha}\widetilde{\beta})(\gamma\delta - \widetilde{\gamma}\widetilde{\delta})\xi$$

and where

$$\mathfrak{a}_N = \prod_{i=i}^{N-1} \left(f^{(i)}_{00} g^{(i)}_{00}\right),$$
$$\mathfrak{b}_N = \prod_{i=1}^{N/2} \frac{f^{(2i-1)}_{01} f^{(2i-1)}_{10} g^{(2i-1)}_{11}}{\left(f^{(2i-1)}_{00}\right)^2 g^{(2i-1)}_{00}} \prod_{i=1}^{N/2-1} \frac{g^{(2i)}_{01} g^{(2i)}_{10} f^{(2i)}_{11}}{\left(g^{(2i)}_{00}\right)^2 f^{(2i)}_{00}},$$
$$\mathfrak{c}_N = \prod_{i=1}^{N/2} \frac{g^{(2i-1)}_{01} g^{(2i-1)}_{10} f^{(2i-1)}_{11}}{\left(g^{(2i-1)}_{00}\right)^2 f^{(2i-1)}_{00}} \prod_{i=1}^{N/2-1} \frac{f^{(2i)}_{01} f^{(2i)}_{10} g^{(2j)}_{11}}{\left(f^{(2i)}_{00}\right)^2 g^{(2i)}_{00}}, \quad (5)$$

and $\alpha' = \alpha + \widetilde{\alpha}$, $\beta' = \beta + \widetilde{\beta}$, $\gamma' = \gamma + \widetilde{\gamma}$, $\delta' = \delta + \widetilde{\delta}$,

$$\widetilde{\alpha} = \frac{f^{(1)}_{10} g^{(1)}_{11}}{f^{(1)}_{00} g^{(1)}_{01}}(1-\alpha), \quad \widetilde{\beta} = \frac{f^{(1)}_{11} g^{(1)}_{10}}{f^{(1)}_{01} g^{(1)}_{00}}(1-\beta),$$
$$\widetilde{\gamma} = \frac{f^{(N-1)}_{11} g^{(N-1)}_{01}}{f^{(N-1)}_{10} g^{(N-1)}_{00}}(1-\gamma), \quad \widetilde{\delta} = \frac{f^{(N-1)}_{01} g^{(N-1)}_{11}}{f^{(N-1)}_{00} g^{(N-1)}_{10}}(1-\delta).$$

When $s = 0$, that is, in the nondeformed case, the polynomial factorizes as in [43] and the largest eigenvalue becomes $\lambda = 1$ as expected.

Dynamical phase transition. From Eq. (4) we can obtain the behavior of the SCGF $\theta_N(s)$ in the large size limit. Since the observables we consider are extensive in system size [cf. Eq. (2)], we have that $a := -\lim_{N\to\infty}(\ln \mathfrak{a}_N)/(Ns)$, $b := -\lim_{N\to\infty}(\ln \mathfrak{b}_N)/(Ns)$, and $c := -\lim_{N\to\infty}(\ln \mathfrak{c}_N)/(Ns)$ exist and are finite. The SCGF then takes the scaling form

$$\theta_N(s) = \vartheta(Ns) + O\left(\frac{1}{N}\right), \quad (6)$$

where the function $\vartheta(\sigma)$ is defined such that $\exp[\vartheta(\sigma)]$ is the leading thermodynamic contribution to the largest root of the polynomial (4) (see [56] for details). The scaling form (6) provides us immediately with system size behavior of the long-time cumulants of $\mathcal{O}_T$

$$\lim_{T\to\infty} \frac{1}{T}\left\langle\!\left\langle \mathcal{O}_T^k \right\rangle\!\right\rangle = (-)^k \frac{d^k}{ds^k}\theta_N\Big|_{s=0} \propto N^k, \quad (7)$$

where $\langle\!\langle\cdot\rangle\!\rangle$ indicates the cumulant. The supralinear dependence on size for $k \geqslant 2$ indicates the presence of a singularity at $s = 0$ in the large size limit.

We can extract explicitly (see [56]) the exact asymptotic of the first few cumulants. From $k = 1$ we get the average observable per unit time

$$\lim_{T\to\infty} \frac{1}{TN}\langle \mathcal{O}_T \rangle = a + \frac{\mu b + \nu c}{2(\mu+\nu) + \alpha\gamma - \beta\delta} + O\left(\frac{1}{N}\right), \quad (8)$$

while from $k = 2$ the corresponding susceptibility

$$\lim_{T\to\infty} \frac{1}{TN} \mathrm{var}\, \mathcal{O}_T = N\Bigg[- \frac{2bc(1-\alpha\gamma) + \mu b^2 + \nu c^2}{2(\mu+\nu) + \alpha\gamma - \beta\delta} + \frac{3(\mu b + \nu c)^2}{[2(\mu+\nu) + \alpha\gamma - \beta\delta]^2} + \frac{2(b+c)(\mu b + \nu c)(2 - \alpha\gamma)}{[2(\mu+\nu) + \alpha\gamma - \beta\delta]^2} - \frac{2(\mu b + \nu c)^2(4 + \mu + \nu - \alpha\gamma)}{[2(\mu+\nu) + \alpha\gamma - \beta\delta]^3}\Bigg] + O(1) \quad (9)$$

with $\mu = \gamma(1-\alpha) + \beta(1-\gamma)$ and $\nu = \delta(1-\alpha) + \alpha(1-\gamma)$.

The scaling function $\vartheta(\sigma)$ has the following properties: (i) at $\sigma = 0$ it vanishes as the corresponding polynomial trivially factorizes [56]; (ii) it is a convex function and $\vartheta''(\sigma)$ admits a global maximum σ^*; (iii) if $(b + c) > 0$ it has the asymptotic behavior

$$\vartheta(\sigma) = \begin{cases} -a\sigma + \ln(\alpha\gamma) + o(1), & \sigma \to \infty \\ -\frac{1}{3}(b + c + 3a)\sigma + \frac{1}{3}\ln(\beta\delta) + o(1), & \sigma \to -\infty \end{cases}$$

[if $(b + c) < 0$ the asymptotic behavior is obtained by $\sigma \to -\sigma$]. We can thus deduce that the SCGF converges to the limit shape

$$\lim_{N\to\infty} \frac{1}{N}\theta_N(s) = \begin{cases} -as, & s > 0 \\ -\frac{1}{3}(b + c + 3a)s, & s < 0 \end{cases} \quad (10)$$

when $(b + c) > 0$ [for $(b + c) < 0$ the shape is obtained by $s \to -s$]. The singularity at $s = 0$ corresponds to a first-order phase transition.

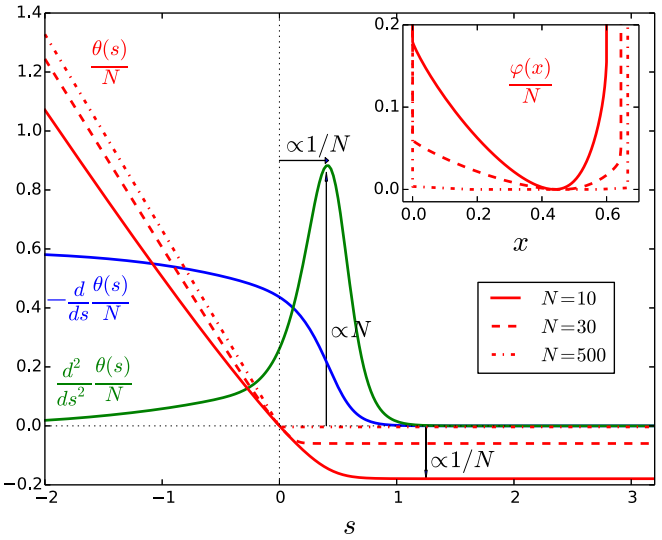

FIG. 2. Dynamical phase transition in the RCA54: Red curves show the exact SCGF $\theta(s)$ for the time-integrated number of up sites [$f_j(n,n') = \frac{1}{2}(n+n')$ and $g_j = 0$ in Eq. (2)] for sizes $N = 10, 30, 500$; the SCGF approaches the singular form (10) for large size. The order parameter, $\lim_{T\to\infty}\langle \mathcal{O}_T e^{-s\mathcal{O}_T}\rangle / TNZ_T(s) = -\theta'(s)/N$ (blue) displays a first-order change between $s < 0$ and $s > 0$, while its susceptibility $\theta''(s)/N$ (green) diverges as N (blue and green curves are for $N = 10$). The first-order singularity at $s_c = 0$ is approached as $1/N$. Inset: Exact rate function $\varphi(x)$ with $x = \mathcal{O}_T/TN$ for sizes $N = 10, 30, 500$. [Parameters are $(\alpha, \beta, \gamma, \delta) = (1/3, 1/8, 1/2, 2/5)$.]

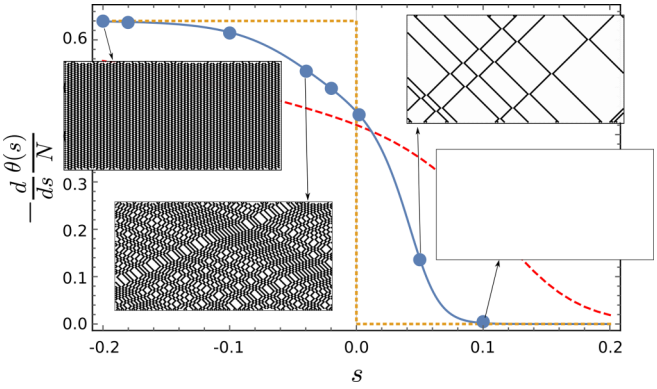

FIG. 3. Sampling of tilted dynamics via Doob transform: The average under Eq. (11) of the observable, $\langle \mathcal{O}_T\rangle_{M_{\text{Doob}}(s)}/TN$ (blue symbols), coincides with the exact value of the order parameter, $-\theta'(s)/N$ (blue curve), as shown for $N = 100$. We show sample trajectories for various values of s: For $s < 0$, trajectories are dense in up sites, thus increasing activity; the leftmost trajectory maximises activity by becoming ordered in space and time - this is the arrangement in the inactive phase for $s < 0$ in the $N \to \infty$ limit (cf. orange/dotted curve). For $s > 0$ trajectories are sparse in up sites, thus reducing activity. (Same observable and parameters as in Fig. 2.)

Figure 2 shows the SCGF for one choice of the observable (the time-integrated number of up sites). As N grows, $\theta_N(s)$ approaches the piecewise linear form (10). The order parameter, $-\theta'(s)/N$, changes from a large value for s negative to one close to zero for s positive, the change becoming discontinuous for $N \to \infty$. The increasing sharpness of the crossover is manifested in the behavior of the susceptibility $\theta''(s)/N$, whose peak grows as N. The value of s at its peak indicates the location of the finite size crossover, which goes as $s_c \propto N^{-1}$. The finite size scaling of the transition point is similar to that expected in the FA model [62–64], while the scaling of the susceptibility is different.

The inset to Fig. 2 shows the rate function $\varphi(x)$ where $x = \mathcal{O}_T/TN$ for various sizes, as obtained from the SCGF via the Legendre transform. As the size increases $\varphi(x)$ progressively broadens. For finite N the broadening is indicative of large fluctuations, and a precursor of the phase transition. In the limit $N \to \infty$, it takes the shape of a flat square well, corresponding to the Maxwell construction due to the first-order coexistence of the two dynamical phases, the inactive one with $x_{\min} = a$ and the active one with $x_{\max} = \frac{1}{3}(b + c + 3a)$ [cf. Eq. (10)] ($\varphi = \infty$ elsewhere). Due to the deterministic nature of the RCA54—and in contrast to facilitated models [24,25,39]—there are no fluctuations within each dynamical phase, which means that for finite N the rate function should have the shape of a "tilted ellipse" [65–67].

Doob transformation and optimal dynamics. The dynamical phase transition above corresponds to a singular change at the level of fluctuations: If the ensemble of trajectories is reweighed by $e^{-s\mathcal{O}_T}$ (the so-called s ensemble [32,39]), there is a singular change in the nature of atypically active trajectories ($s < 0$) to atypically inactive ones ($s > 0$). These reweighed ensembles can be sampled from the original dynamics by post-processing, but this is exponentially costly in T. However, they can be optimally accessed in terms of an "auxiliary" [68] or "driven" [69] Markov process, by means of a so-called *generalized Doob transformation* (see also [70–75]). The generalized Doob transform gives the optimal way to generate rare dynamical events. That is, any other manner is exponentially suppressed in time and volume. From the matrix product construction of the leading eigenvector of $M(s)$ we can obtain the exact long-time Doob operator [68,69,73]:

$$M_{\text{Doob}} = \frac{1}{\lambda(s)}\mathcal{L}M(s)\mathcal{L}^{-1}, \tag{11}$$

where $\mathcal{L}$ is a diagonal operator formed out of components of the leading *left* eigenvector $\boldsymbol{q}$ of $M(s)$, i.e., $\mathcal{L}_{\mathbf{n},\mathbf{n}'} := \delta_{\mathbf{n},\mathbf{n}'}q_{\mathbf{n}}$. The exact matrix product construction of $\boldsymbol{q}$ is given in [56]. The operator (11) is a Markov matrix for a stochastic dynamics whose trajectories are guaranteed to coincide—for long times–with those of the s ensemble of the original M [68,69,71–73]. Figure 3 shows how M_{Doob} allows one to sample the fluctuations of the RCA54 parametrized by s in an optimal way. We see that both the active and inactive phases on their own seem not to fluctuate, and the probability tends in the large size limit to a step: A delta function at the minimal possible value of the observable, another one at the maximal value, and the flat part that connects the two. The individual phases therefore do not or cannot fluctuate, and the SCGF becomes piecewise linear as in Fig. 2. We see this as a consequence of the bulk deterministic character of the model. Consequently, the Doob operator amounts to a nontrivial modification only

of the boundary probabilities, which in M_{Doob} depend on the configuration of the whole lattice. For details see [56].

Conclusion. We studied the statistics of a general class of dynamical observables in a cellular automaton with stochastic boundary driving. We provided an exact expression of their scaled cumulant generating functions by means of an inhomogeneous matrix product expression for the leading eigenvector of the corresponding tilted Markov operator. Our results give a precise analytical description of the phase transition between active and inactive dynamical phases observed in a wide range of other models.

We foresee extensions of our work here in several directions, including computing the large deviation statistics of currents, and even the complete "level 2.5" statistics for the empirical measure and fluxes [76–80]. The analytic inhomogeneous matrix ansatz introduced here could also be used to address similar questions in more complicated models, for instance for cellular automata with asymmetric constraints, and for systems with stochastic dynamics in the bulk.

Acknowledgments. This work has been supported by Advanced Grant No. 694544–OMNES of the European Research Council (ERC), Grants No. N1-0025 and No. N1-0055 of the Slovenian Research Agency (ARRS), EPSRC programme Grant No. EP/P009565/1, EPSRC Grant No. EP/R04421X/1, and The Leverhulme Trust Grant No. RPG-2018-181.

[1] B. Derrida, J. Stat. Mech. (2007) P07023.
[2] K. Mallick, Phys. A: Stat. Mech. Appl. **418**, 17 (2015), Proceedings of the 13th International Summer School on Fundamental Problems in Statistical Physics .
[3] C. L. Henley, Annu. Rev. Condens. Matter Phys. **1**, 179 (2010).
[4] J. T. Chalker, in *Topological Aspects of Condensed Matter Physics*, edited by C. Chamon, M. Goerbig, R. Moessner, and L. Cugliandolo, Lecture Notes of the Les Houches Summer School Vol. 103 (Oxford University Press, Oxford, 2017), p. 123.
[5] F. Ritort and P. Sollich, Adv. Phys. **52**, 219 (2003).
[6] J. P. Garrahan, P. Sollich, and C. Toninelli, in *Dynamical Heterogeneities in Glasses, Colloids, and Granular Media*, edited by L. Berthier, G. Biroli, J.-P. Bouchaud, L. Cipelletti, and W. van Saarloos, International Series of Monographs on Physics, (Oxford University Press, Oxford, UK, 2011).
[7] M. van Horssen, E. Levi, and J. P. Garrahan, Phys. Rev. B **92**, 100305(R) (2015).
[8] A. Smith, J. Knolle, D. L. Kovrizhin, and R. Moessner, Phys. Rev. Lett. **118**, 266601 (2017).
[9] N. Shiraishi and T. Mori, Phys. Rev. Lett. **119**, 030601 (2017).
[10] Z. Lan, M. van Horssen, S. Powell, and J. P. Garrahan, Phys. Rev. Lett. **121**, 040603 (2018).
[11] C. Turner, A. Michailidis, D. Abanin, M. Serbyn, and Z. Papić, Nat. Phys. **14**, 745 (2018).
[12] A. Nahum, J. Ruhman, S. Vijay, and J. Haah, Phys. Rev. X **7**, 031016 (2017).
[13] C. W. von Keyserlingk, T. Rakovszky, F. Pollmann, and S. L. Sondhi, Phys. Rev. X **8**, 021013 (2018).
[14] D. A. Rowlands and A. Lamacraft, Phys. Rev. B **98**, 195125 (2018).
[15] X. Chen and T. Zhou, Phys. Rev. B **100**, 064305 (2019).
[16] S. Gopalakrishnan, Phys. Rev. B **98**, 060302(R) (2018).
[17] M. Knap, Phys. Rev. B **98**, 184416 (2018).
[18] M. C. Tran, A. Y. Guo, Y. Su, J. R. Garrison, Z. Eldredge, M. Foss-Feig, A. M. Childs, and A. V. Gorshkov, Phys. Rev. X **9**, 031006 (2019).
[19] S. Gopalakrishnan, D. A. Huse, V. Khemani, and R. Vasseur, Phys. Rev. B **98**, 220303(R) (2018).
[20] I. Lesanovsky and J. P. Garrahan, Phys. Rev. Lett. **111**, 215305 (2013).
[21] A. Urvoy, F. Ripka, I. Lesanovsky, D. Booth, J. P. Shaffer, T. Pfau, and R. Löw, Phys. Rev. Lett. **114**, 203002 (2015).
[22] M. M. Valado, C. Simonelli, M. D. Hoogerland, I. Lesanovsky, J. P. Garrahan, E. Arimondo, D. Ciampini, and O. Morsch, Phys. Rev. A **93**, 040701(R) (2016).
[23] V. Lecomte, C. Appert-Rolland, and F. van Wijland, J. Stat. Phys. **127**, 51 (2007).
[24] J. P. Garrahan, R. L. Jack, V. Lecomte, E. Pitard, K. van Duijvendijk, and F. van Wijland, Phys. Rev. Lett. **98**, 195702 (2007).
[25] J. P. Garrahan, R. L. Jack, V. Lecomte, E. Pitard, K. van Duijvendijk, and F. van Wijland, J. Phys. A **42**, 075007 (2009).
[26] H. Touchette, Phys. Rep. **478**, 1 (2009).
[27] C. Appert-Rolland, B. Derrida, V. Lecomte, and F. van Wijland, Phys. Rev. E **78**, 021122 (2008).
[28] C. P. Espigares, P. L. Garrido, and P. I. Hurtado, Phys. Rev. E **87**, 032115 (2013).
[29] R. L. Jack, I. R. Thompson, and P. Sollich, Phys. Rev. Lett. **114**, 060601 (2015).
[30] D. Karevski and G. M. Schütz, Phys. Rev. Lett. **118**, 030601 (2017).
[31] T. Oakes, S. Powell, C. Castelnovo, A. Lamacraft, and J. P. Garrahan, Phys. Rev. B **98**, 064302 (2018).
[32] L. O. Hedges, R. L. Jack, J. P. Garrahan, and D. Chandler, Science **323**, 1309 (2009).
[33] T. Speck, A. Malins, and C. P. Royall, Phys. Rev. Lett. **109**, 195703 (2012).
[34] J. K. Weber, R. L. Jack, and V. S. Pande, J. Am. Chem. Soc. **135**, 5501 (2013).
[35] Y. Baek, Y. Kafri, and V. Lecomte, Phys. Rev. Lett. **118**, 030604 (2017).
[36] J. P. Garrahan and I. Lesanovsky, Phys. Rev. Lett. **104**, 160601 (2010).
[37] A. Bobenko, M. Bordemann, C. Gunn, and U. Pinkall, Commun. Math. Phys. **158**, 127 (1993).
[38] G. H. Fredrickson and H. C. Andersen, Phys. Rev. Lett. **53**, 1244 (1984).
[39] J. P. Garrahan, Physica A **504**, 130 (2018).
[40] S. Takesue, Phys. Rev. Lett. **59**, 2499 (1987).
[41] T. Prosen and C. Mejía-Monasterio, J. Phys. A **49**, 185003 (2016).
[42] A. Inoue and S. Takesue, J. Phys. A **51**, 425001 (2018).
[43] T. Prosen and B. Buča, J. Phys. A **50**, 395002 (2017).
[44] K. Klobas, M. Medenjak, T. Prosen, and M. Vanicat, Commun. Math. Phys. (2019), doi: 10.1007/s00220-019-03494-5.
[45] B. Derrida and J. L. Lebowitz, Phys. Rev. Lett. **80**, 209 (1998).
[46] S. Prolhac, J. Phys. A **43**, 105002 (2010).
[47] J. de Gier and F. H. L. Essler, Phys. Rev. Lett. **107**, 010602 (2011).

[48] M. Gorissen, A. Lazarescu, K. Mallick, and C. Vanderzande, Phys. Rev. Lett. **109**, 170601 (2012).
[49] N. Crampé, E. Ragoucy, V. Rittenberg, and M. Vanicat, Phys. Rev. E **94**, 032102 (2016).
[50] H. Hinrichsen, J. Phys. A: Math. Gen. **29**, 3659 (1996).
[51] J. de Gier and B. Nienhuis, Phys. Rev. E **59**, 4899 (1999).
[52] A. Lapolla and A. Godec, New J. Phys. **20**, 113021 (2018).
[53] S. Großkinsky, G. M. Schütz, and R. D. Willmann, J. Stat. Phys. **128**, 587 (2007).
[54] T. Bodineau and M. Lagouge, J. Stat. Phys. **139**, 201 (2010).
[55] O. Hirschberg, D. Mukamel, and G. M. Schütz, J. Stat. Mech.: Theor. Exp. (2015) P11023.
[56] See Supplemental Material at http://link.aps.org/supplemental/10.1103/PhysRevE.100.020103 for precise definition of the model and its (tilted) Markov matrix, for details on the inhomogeneous cancellation scheme with the matrix product ansatz for the left and right leading tilted eigenvector together with explicit exact solutions of the boundary equations, and for explicit construction of the Doob transform.
[57] B. Derrida, M. R. Evans, V. Hakim, and V. Pasquier, J. Phys. A **26**, 1493 (1993).
[58] M. Vanicat, J. Stat. Phys. **166**, 1129 (2017).
[59] M. Vanicat, Nucl. Phys. B **929**, 298 (2018).
[60] C. Finn and M. Vanicat, J. Stat. Mech.: Theor. Exp. (2017) 023102.
[61] N. Crampé, E. Ragoucy, and D. Simon, J. Phys. A **44**, 405003 (2011).
[62] T. Bodineau, V. Lecomte, and C. Toninelli, J. Stat. Phys. **147**, 1 (2012).
[63] T. Bodineau and C. Toninelli, Commun. Math. Phys. **311**, 357 (2012).
[64] T. Nemoto, R. L. Jack, and V. Lecomte, Phys. Rev. Lett. **118**, 115702 (2017).
[65] A. N. Jordan and E. V. Sukhorukov, Phys. Rev. Lett. **93**, 260604 (2004).
[66] N. Lambert, F. Nori, and C. Flindt, Phys. Rev. Lett. **115**, 216803 (2015).
[67] K. Brandner, V. F. Maisi, J. P. Pekola, J. P. Garrahan, and C. Flindt, Phys. Rev. Lett. **118**, 180601 (2017).
[68] R. L. Jack and P. Sollich, Prog. Theor. Phys. Suppl. **184**, 304 (2010).
[69] R. Chetrite and H. Touchette, Ann. Henri Poincaré **16**, 2005 (2015).
[70] V. S. Borkar, S. Juneja, and A. A. Kherani, Commun. Inf. Syst. **3**, 259 (2003).
[71] R. Chetrite and H. Touchette, J. Stat. Mech. (2015) P12001.
[72] R. L. Jack and P. Sollich, Eur. Phys. J.: Spec. Top. **224**, 2351 (2015).
[73] J. P. Garrahan, J. Stat. Mech.: Theor. Exp. (2016) 073208.
[74] F. Carollo, J. P. Garrahan, I. Lesanovsky, and C. Pérez-Espigares, Phys. Rev. A **98**, 010103(R) (2018).
[75] B. Derrida and T. Sadhu, J. Stat. Phys. **176**, 773 (2019).
[76] C. Maes and K. Netocny, Europhys. Lett. **82**, 30003 (2008).
[77] L. Bertini, A. Faggionato, and D. Gabrielli, Stochastic Process. Appl. **125**, 2786 (2015).
[78] A. C. Barato and R. Chetrite, J. Stat. Phys. **160**, 1154 (2015).
[79] J. Hoppenau, D. Nickelsen, and A. Engel, New J. Phys. **18**, 083010 (2016).
[80] L. Bertini, R. Chetrite, A. Faggionato, and D. Gabrielli, Ann. Henri Poincaré **19**, 3197 (2018).